3,4-Dihydroxy-L-Phenylalanine as a Novel Covalent Linker of Extracellular Matrix Proteins to Polyacrylamide Hydrogels with a Tunable Stiffness

Wouters, Olaf Y.; Ploeger, Diana T. A.; van Putten, Sander M.; Bank, Ruud A.

Published in:
Tissue Engineering. Part C: Methods

DOI:
10.1089/ten.tec.2015.0312

Publication date:
2016

TISSUE ENGINEERING: Part C
Volume 22, Number 2, 2016

DOI: 10.1089/ten.tec.2015.0312

termis
Tissue Engineering
& Regenerative Medicine
International Society

METHODS ARTICLE

3,4-Dihydroxy-L-Phenylalanine as a Novel Covalent Linker of Extracellular Matrix Proteins to Polyacrylamide Hydrogels with a Tunable Stiffness

Olaf Y. Wouters, MSc,[1] Diana T.A. Ploeger, MSc,[1] Sander M. van Putten, PhD,[1,2] and Ruud A. Bank, PhD[1]

Cells acquire mechanical information from their surrounding and convert this into biochemical activity. The concept and mechanism behind this cellular mechanosensing and mechanotransduction are often studied by means of two-dimensional hydrogels. Polyacrylamide hydrogels (PAAMs) offer chemical, mechanical, and optical advantages but due to their inert surface do not allow protein and cell adherence. Several cross-linkers have been used to functionalize the surface of PAAMs with extracellular matrix (ECM) proteins to enable cell culture. However, the most commonly used cross-linkers are either unstable, expensive, or laborious and often show heterogeneous coating or require PAAM modification. Here, we introduce 3,4-dihydroxy-L-phenylalanine (L-DOPA) as a novel cross-linker that can functionalize PAAMs with ECM without the above-mentioned disadvantages. A homogenous collagen type I and fibronectin coating was observed after L-DOPA functionalization. Fibroblasts responded to differences in PAAMs' stiffness; morphology, cell area, and protein localization were all affected as expected, in accordance with literature where other cross-linkers were used. In conclusion, L-DOPA can be used as a cross-linker between PAAMs and ECM and represents a novel, straightforward, nonlaborious, and robust method to functionalize PAAMs for cell culture to study cell mechanosensing.

Introduction

Cells sense and respond to external mechanical signals from their environment and convert this mechanical stimulus into biochemical activity, a process known as mechanosensing and mechanotransduction.[1] Indeed, cells actively sense their environment by applying forces to the surrounding substrate at the site of adhesion.[2] An increase in substrate stiffness directly influences cell morphology as stiffer materials lead to more cell spreading.[3] Cells also migrate more easily on and toward stiffer materials, a phenomenon called durotaxis.[4,5] Furthermore, cells generally proliferate faster on a stiff substrate,[6] and substrate stiffness affects stem cell lineage differentiation.[7,8]

To study the effect of substrate stiffness on cells *in vitro*, polyacrylamide hydrogels (PAAMs) have been used for years as elastomers with a pretunable stiffness.[5,9–11] PAAMs offer chemical, optical, and mechanical advantages. PAAMs are translucent and nonfluorescent, which enables their use in immunohistochemistry and fluorescence microscopy. PAAMs also show linear deformation in response to mechanical load and show rapid and complete recovery after release.[10] Furthermore, PAAMs offer linear elasticity independent of applied strain,[12] enabling the verification of PAAMs elastic moduli by fitting force retraction curves obtained with an atomic force microscope (AFM) with a linear Hertz model.[13,14] Extremely low moduli mimicking organ stiffness *in vivo* (<5 kPa)[15] can be obtained by varying the ratio between acrylamide and bisacrylamide without introducing changes in the surface chemistry.

Despite excellent optical, chemical, and mechanical properties, PAAMs are biologically inert and require surface functionalization to facilitate cell adhesion. In the past, a variety of cross-linkers have been used to couple protein to the surface of PAAMs. Sulfo-SANPAH (sulfosuccinimidyl 6-(4′-azido-2′-nitrophenylamino)hexanoate), a chemical cross-linker and golden standard as of today, is used to functionalize the surface of PAAMs with extracellular matrix (ECM) proteins or peptides for cell adherence. Sulfo-SANPAH couples to PAAMs through a photo-activatable nitrophenyl azide and can bind protein through an amine-reactive *N*-hydroxysuccinimide ester. Sulfo-SANPAH is an expensive reagent that due to its poor solubility, limited stability, and short shelf life can show variations in cross-linking, which leads to heterogeneous ECM coating.[15,16] This results in poor, heterogeneous, aberrant, or no adhesion of cells.

[1]Department of Pathology and Medical Biology, University of Groningen, University Medical Center Groningen, Groningen, The Netherlands.
[2]Synvolux Therapeutics, Groningen, The Netherlands.

Other used cross-linkers are dependent on polyacrylamide mixture modifications[10,16]: 1-ethyl-3-(3-dimethylaminopropyl) carbodiimide hydrochloride can only couple protein to PAAMs when acrylic acid is incorporated into the hydrogel because it depends on a free carboxylic acid group to form a stable amide bond. Another used cross-linker, 6-acrylaminohexylaminohexanoic acid *N*-succinimidyl ester (N6) needs to be incorporated directly into PAAMs and these modifications may influence hydrogel stiffness, stability and integrity. The synthesis of N6 is another limitation as it can only be formed through a multistep chemical reaction, which is hard to implement for most biologically oriented laboratories. Alternatives such as polydimethylsiloxane (PDMS) are a less desirable choice for studying cell mechanosensing due to nonlinear mechanical behavior.[17]

Clearly, the need for a straightforward protocol to functionalize PAAMs for cell culture to study mechanosensing and mechanotransduction *in vitro* remains. In this article, 3,4-dihydroxy-L-phenylalanine (L-DOPA), the dopamine precursor and key compound in mussel byssus adhesion,[18–20] is proposed to substitute said cross-linkers to couple ECM proteins to unmodified PAAMs with different substrate stiffness. L-DOPA is a nontoxic compound, which is extensively used in the clinic for the treatment of Parkinson's disease and dopamine-responsive dystonia and is considered biocompatible. As shown by Lee *et al.*, L-DOPA can bind to various materials such as steel, titanium, polystyrene, and PDMS.[21] L-DOPA has also been used as a cell-adhesion molecule in serum-free cell cultures as discussed by Wan-Geun La *et al.*[22] L-DOPA is more economic in use compared to sulfo-SANPAH and is chemically stable in the supplied powder form. We combined the excellent optical, chemical and mechanical properties of PAAMs with the remarkable binding properties of L-DOPA to functionalize PAAMs for cell culture and briefly compare our functionalization method with sulfo-SANPAH. Using this method, we offer a novel, easy, and robust *in vitro* model to study the effect of substrate stiffness on the biology of cells. We validated our model by studying the effect of substrate stiffness on human fetal fibroblasts using the following characteristics: cell adherence, cell area, the incorporation of alpha smooth muscle actin (αSMA) into stress fibers, the localization of vinculin in focal adhesions, and the translocation of Yes-associated protein (YAP) into the nucleus.

Materials and Methods

Preparation of PAAMs

PAAMs were prepared between a chemically modified glass plate and a glass coverslip, a slight modification of a method first described by Pelham and Wang.[10] The glass plate was sterilized in an autoclave, followed by immersion in 99.9% ethanol for 15 min. To prevent PAAM adhesion to the underlying glass plate, it was incubated with dichlorodimethylsilane (8034520; Merck, Darmstadt, Germany) for 5 min, wiped clean and washed gently with sterile water afterward. Glass coverslips (Ø 15 mm; VWR, Amsterdam, The Netherlands) were, to covalently link PAAMs, pretreated for 3 min with a freshly prepared solution of 99.9% ethanol containing 0.5% (v/v) 3-(trimethoxysilyl)propyl methacrylate (M6514; Sigma, St. Louis, MO) and 0.3% (v/v) glacial acetic acid. After incubation, the mixture was carefully aspirated and coverslips were washed twice with 99.9% ethanol to remove residual reagents.

PAAMs with mechanical properties mimicking *in vivo* tissue stiffness were prepared by varying the ratio between 40% acrylamide solution (#161-0140; BioRad, Veenendaal, The Netherlands) and 2% bisacrylamide solution (#161-0142; BioRad) in 10 mM 4-(2-hydroxyethyl)-1-piperazineethanesulfonic acid buffer (HEPES, H0887; Sigma-Aldrich) as depicted in Table 1. The polymerization catalyst *N*,*N*,*N*′,*N*′-tetramethylethylenediamine (#161-0800; BioRad) was added to the mixture in a final concentration of 0.15%. This solution was deoxygenated under argon for 30 min. Without deoxygenation, large variations in hydrogel stiffness, homogeneity, and polymerization speed were observed. After deoxygenation, the (bis)acrylamide solution was gently mixed with ammonium persulfate (APS; A3678, Sigma-Aldrich; Table 1). APS addition was quickly followed by pipetting the polymerizing solution onto the glass plate and has to be done in rapid succession, placing a coverslip on top. PAAMs covalently linked to the glass coverslips were left to polymerize for 15–30 min before carefully flipping them with a needle and tweezers and placed into 24-well culture well plates. To cease the polymerization process and remove leftover acrylamide and bisacrylamide monomers, the PAAMs were washed twice with phosphate buffered saline (PBS) and stored in PBS in the fridge until further use. Hydrogel surface creasing of soft gels was prevented by adapting acrylamide and bisacrylamide concentrations as described by Saha *et al.*[23]

Atomic force microscopy

The mechanical properties of the PAAMs were measured using a Bruker BioScope Catalyst AFM (Bruker UK Limited, Coventry, United Kingdom) in contact in fluid mode in PBS. Triangular silicon nitride cantilevers (NP10; Bruker UK Limited) with nominal spring constants of 0.06 N/m were used. Cantilever spring constants were determined and calibrated on glass at the beginning of each experiment. The stiffness of each PAAM was measured at three random topographic locations

Table 1. Acryl/Bisacrylamide Volumes for 24-Well Plate Coverslips

Measured E *(Young's modulus, kPa)*	*2*	*4*	*12*	*26*	*50*	*92*
40% acrylamide (μL)	75	187.5	187.5	187.5	300	300
2% bisacrylamide (μL)	60	27	58	118	58.5	75.5
10 mM HEPES (μL)	763.5	684	653	593	540	523
TEMED (μL)	1.5	1.5	1.5	1.5	1.5	1.5
APS (μL)	100	100	100	100	100	100
Total (μL)	1000	1000	1000	1000	1000	1000

APS, ammonium persulfate; HEPES, 4-(2-hydroxyethyl)-1-piperazineethanesulfonic acid buffer; TEMED, *N*,*N*,*N*′,*N*′-tetramethylethylenediamine.

per hydrogel to assure homogeneity and assessed by 20 indentations per location. The stiffness was validated by repeated measurements per day (triple hydrogels) and by repeated experiments at different days ($n=3$) to validate reproducibility. The Young's modulus was obtained retrospectively by fitting obtained force retraction curves with a linear Hertz model.[13,14]

L-DOPA to functionalize the surface of PAAMs

The catecholamine L-DOPA (D9628; Sigma-Aldrich) was used to functionalize the surface of PAAMs. L-DOPA was dissolved in 10 mM Tris buffer (pH 10) at a final concentration of 2 mg/mL unless otherwise specified and left to dissolve for 30 min in the dark. After dissolving, the L-DOPA solution was sterilized through a 0.20 μm surfactant-free cellulose acetate filter, and PAAMs were incubated with 250 μL of L-DOPA for 30 min in the dark, followed by two washes with PBS to remove any residual unbound L-DOPA. L-DOPA-coated hydrogels were functionalized with 250 μL of either a 20 μg/mL fibronectin (F1141; Sigma-Aldrich) or a 40 μg/mL rat-tail tendon collagen type I (354249; BD Bioscience, San Jose, CA) solution in PBS at 37°C for 2 h, unless stated otherwise. After incubation, gels were washed with PBS to remove any unbound ECM components. During optimization experiments, the time and concentration of both L-DOPA and collagen I were varied to determine L-DOPA and collagen I binding dynamics. A schematic representation of L-DOPA as a cross-linker in our PAAM model is depicted in Figure 1.

Sulfo-SANPAH

To compare our method with sulfo-SANPAH, we coated PAAMs with either sulfo-SANPAH or L-DOPA (2 mg/mL L-DOPA in 10 mM Tris buffer and filtered before use, as described in previous paragraph) before collagen I functionalization. In brief, PAAMs were overlaid with 200 μL of a 0.5 mg/mL (1 mM) sulfo-SANPAH in 50 mM HEPES solution and incubated under a 365 nm UV lamp for 5 min, as described by Pelham and Wang.[10,24] Next, PAAMs were washed three times with 50 mM HEPES and incubated with collagen I for 2 h at 37°C.

Immunofluorescence and quantification of collagen type I coating on PAAMs

To visualize collagen type I and fibronectin bound to the surface of the PAAMs through L-DOPA or sulfo-SANPAH, gels were incubated for 30 min with (1) 10% goat serum or (2) 10% donkey serum followed by incubation with either (1) mouse monoclonal antibody to collagen type I (ab90395; Abcam, Cambridge, United Kingdom; 1:5000 in PBS) or (2) rabbit polyclonal antibody to fibronectin (ab2413; Abcam; 1:1000 in PBS) for 2 h. Gels were washed with PBS and incubated with (1) goat-anti-mouse IRDye 800 CW (610–132-121: Rockland, Limerick, PA) or (2) donkey-anti-rabbit IRDye 680 CW (926-68073; Rockland; both 1:500 in PBS) for 1 h followed by three washes with PBS. ECM coating was visualized at infrared wavelength (780 nm for collagen I, 680 nm for fibronectin) using the Odyssey Infrared Imaging System (LI-COR, Lincoln, NE). Collagen I and fibronectin staining were quantified using the supplied LI-COR image studio software for Windows, version 4.0.21.

Cell culture

To determine cell adhesion, human dermal fetal fibroblasts (WS1 CRL-1502; ATCC, Teddington, United Kingdom) were pretreated with 10 μg/mL mitomycin C (M4287; Sigma-Aldrich) for 2 h. Mitomycin C forms cross-links between the DNA strands and therefore inhibits DNA synthesis and proliferation. Fibroblasts were seeded on L-DOPA/collagen type I-functionalized PAAMs with a density of 1000 cells/cm^2 to avoid confluent cell–cell contact and cultured in Eagle's minimum essential medium (Thermo Scientific, Waltham, MA) supplemented with 10% filtered heat-inactivated fetal calf serum (SV3016; Thermo Scientific, Waltham, MA), 1% penicillin/streptomycin, and 1% L-glutamine (both from Sigma-Aldrich) under 20% O_2 and 5% CO_2 at 37°C. For cell adherence, fibroblasts were cultured for 24 h on plain PAAMs, PAAMs coated with only collagen type I or PAAMs functionalized with L-DOPA and collagen type I. For immunofluorescence detection of cell area and protein (trans)location, fibroblasts were cultured on PAAMs functionalized with L-DOPA/collagen type I. After either 24 h (cell adhesion) or 48 h (cell area, protein [trans]location), fetal fibroblasts were washed twice with PBS and fixated with 2% paraformaldehyde (PFA) at 4°C for 15 min.

Cell adhesion and area

To assess cell adherence, PFA-fixated cells cultured for 24 h on functionalized gels were incubated with 4′,6-diamidino-2-phenylindole (DAPI; D9542; Sigma-Aldrich) for nuclear staining (1:5000 in PBS). To assess cell area, fibroblasts cultured on either L-DOPA–collagen I or L-DOPA–fibronectin-functionalized PAAMs were fixated after 48 h. Next cells were stained with DAPI (1:5000 in PBS) and phalloidin tetramethylrhodamine B isothiocyanate (phalloidin-TRITC; P1951; Sigma-Aldrich; 1:1000 in PBS; F-actin staining) for 10 min, followed by three washes with PBS supplemented with 0.5% Tween-20. Slides were mounted in Citifluor (Agar Scientific, Essex, United Kingdom).

Images for cell adherence and cell area were obtained with a TissueFAXS equipped with a Pixelfly camera and a 10× objective. For cell adherence, 36 field of views (FOVs) and for cell area 25 FOVs were acquired per stiffness and these images were automatically stitched together by the TissueGnostics TissueFAXS software. Both cell adherence and cell area

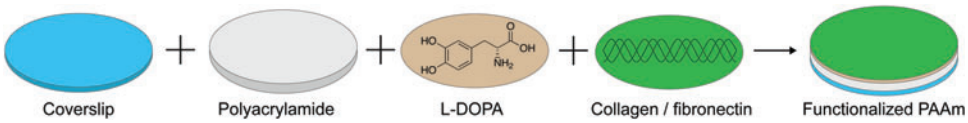

FIG. 1. Schematic representation of the PAAM–L-DOPA–ECM construct. A glass coverslip with covalently attached PAAM is coated with L-DOPA, after which the PAAM is functionalized with ECM proteins (collagen I, fibronectin). ECM, extracellular matrix; L-DOPA, 3,4-dihydroxy-L-phenylalanine; PAAM, polyacrylamide hydrogel. Color images available online at www.liebertpub.com/tec

experiments were repeated four times and analyzed using the Leica NuanceFX software. To analyze the cell area, stitched images were converted to spectral cubes to unmix fluorescence background from phalloidin staining. Using the threshold segmentation function, cell area was measured in pixels. Each cell was checked and manually corrected using the draw/erase function if necessary. At least 100 cells were measured per hydrogel. By using the TissueFAXS provided scale bar, the measured pixels were subsequently converted to μm^2.

Immunofluorescent staining for F-actin, αSMA, vinculin, and YAP in fetal fibroblasts on PAAMs

To visualize αSMA, vinculin, and YAP, PFA-fixated fibroblasts were permeabilized with 0.5% Triton X-100 (108643; Merck) for 10 min and incubated with 10% goat serum for 1 h. Next, fibroblasts were incubated for 2 h at room temperature (RT) with (1) mouse monoclonal to αSMA (Clone 1A4; DAKO, Glosstrup, Denmark; 1:100), (2) mouse monoclonal to vinculin (hVIN-1; Sigma-Aldrich; 1:1000), or (3) rabbit polyclonal to YAP (sc-15407; Santa Cruz, Dallas, TX; 1:1000) in PBS containing 2.2% bovine serum albumin (BSA). After three washes with PBS, fibroblasts were incubated with biotinylated (1) IgG2a-specific goat-anti-mouse (1080-08; SouthernBiotech, Birmingham, AL; 1:250), (2) IgG1-specific goat-anti-mouse–biotin (1070-08; SouthernBiotech; 1:250), or (3) polyclonal goat-anti-rabbit–biotin (E0432; DAKO, Glosstrup, Denmark; 1:250), diluted in PBS containing 2.2% BSA for 1 h at RT. Cells were washed three times with PBS and incubated with streptavidin-CY5 (Invitrogen, Grand Island, NY; 1:250) in PBS containing DAPI (1:5000) for 30 min. After three washes with PBS, slides were mounted in Citifluor (Agar Scientific).

αSMA, vinculin, and YAP were visualized using a Leica DMI 6000 equipped SP8 confocal microscope using a 40× oil objective. Overlays of confocal z-stacks were created using ImageJ with the FIJI image processing package.[25]

Statistics

All data are represented as mean ± standard error of the mean. All experiments were analyzed using GraphPad Prism, version 6 (GraphPad Software, La Jolla, CA) either by one-way or two-way ANOVA, followed by Bonferroni *post hoc* analysis. Values of $p < 0.05$ were considered to be statistically significant.

Results

Characterization of PAAMs functionalized with L-DOPA

We obtained PAAMs with mechanical properties that match the physiological stiffness of different tissues by varying the ratio between acrylamide and bisacrylamide (Fig. 2). A key step to obtain PAAM stability, homogeneity, and reproducibility is deoxygenation: we obtained excellent results when we used the inert gas argon to deoxygenize our acrylamide/bisacrylamide solutions. Our PAAMs derived from mixtures mimicking the *in vivo* stiffness (Young's modulus between 2 and 92 kPa) showed a high reproducibility with low variation (Fig. 2).

Next, we functionalized PAAMs with collagen type I using the catecholamine L-DOPA. Because directly quantifying L-DOPA adherence to the PAAM surface is difficult, we have

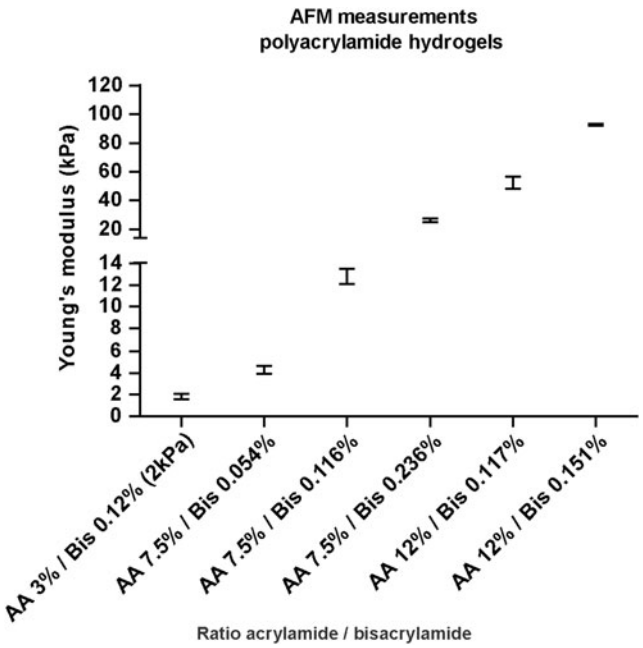

FIG. 2. Stiffness of PAAM hydrogels. Mechanical properties of PAAMs were obtained by atomic force microscopy in contact in fluid mode in phosphate buffered saline with triangular silicon nitride cantilevers. Data shown represent three experiments conducted separately, each consisting of triple hydrogels. Each hydrogel was measured at three different topographic locations to validate PAAM homogeneity.

indirectly measured L-DOPA through collagen I adherence using the highly sensitive LI-COR Odyssey Infrared Imaging System. Coating of PAAM with collagen type I, using L-DOPA as a cross-linker, is time and concentration dependent (Fig. 3A, B). We observed complete and homogenous collagen type I coating of PAAMs after 10 min of incubation with L-DOPA at RT (Fig. 3A) at the optimal L-DOPA concentration (2 mg/mL; Fig. 3B). Collagen I adhered in a fast and efficient manner to L-DOPA; no detectable increase in collagen type I adherence at the surface of L-DOPA-functionalized hydrogels was detected after 30 min of collagen incubation (Fig. 3C). When L-DOPA is used at the optimal concentration of 2 mg/mL in 10 mM Tris, collagen is the limiting factor in collagen surface density (Fig. 3D). PAAMs coated with L-DOPA and functionalized with collagen I showed no significant differences in collagen density between hydrogels with different degrees of stiffness (Fig. 3E). Without L-DOPA treatment, collagen type I could not bind to the PAAMs (Fig. 3E). Furthermore, we see a marked improvement in collagen I functionalization when comparing L-DOPA with sulfo-SANPAH (Fig. 3F). Note that sulfo-SANPAH not only shows less collagen I adherence compared to L-DOPA but also shows a more heterogeneous collagen I coating. Adhesion of ECM to L-DOPA-functionalized PAAMs was also validated with fibronectin (Fig. 4D) where similar results as collagen I were obtained (Fig. 3E).

Effect of substrate stiffness on cell adherence and cell spreading

To validate our method, human fetal fibroblasts pre-incubated with mitomycin C were seeded onto plain PAAMs,

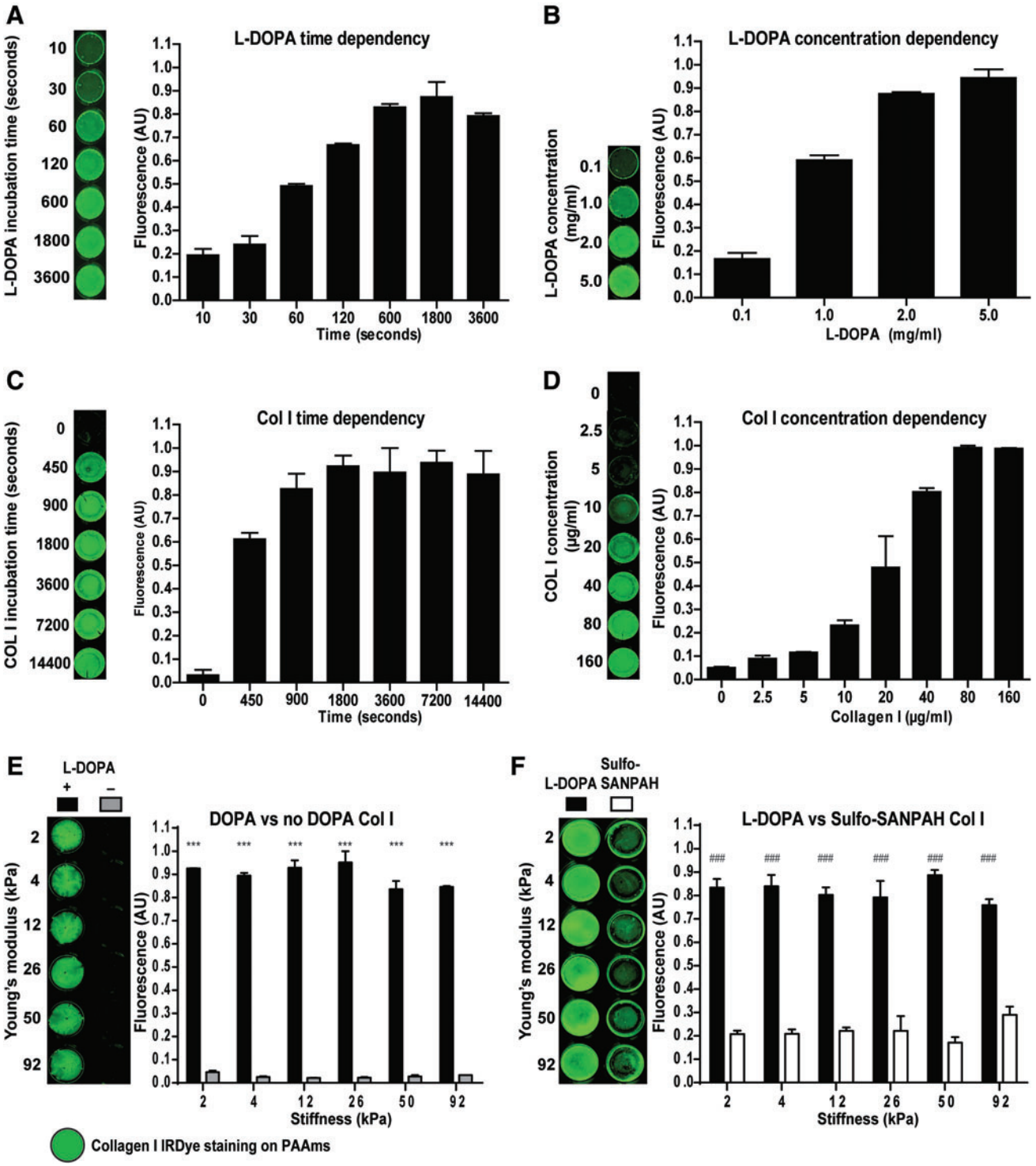

FIG. 3. Polyacrylamide surface functionalization with collagen type I using L-DOPA. Collagen I functionalization was visualized using the LI-COR Odyssey infrared imaging system. Computed pseudocolored images of collagen I coating of PAAMs are shown *left* of the quantification graphs. L-DOPA shows **(A)** time- and **(B)** concentration-dependent functionalization of PAAMs. **(C)** At the optimal L-DOPA concentration (2 mg/mL in 10 mM Tris), collagen I adhered in a time- and **(D)** concentration-dependent manner to the L-DOPA-functionalized PAAMs. **(E)** Without L-DOPA functionalization, collagen I did not adhere to the inert PAAMs (*grey bars*). L-DOPA–collagen I functionalization showed no significant differences between hydrogels of different stiffness (*black bars*). **(F)** L-DOPA (*black bars*) shows a significant enhancement in collagen I adherence compared to sulfo-SANPAH (*white bars*). Statistics were performed by two-way ANOVA with Bonferroni *post hoc* test. ***Significant difference between hydrogels functionalized with L-DOPA and collagen I or collagen I alone, p-value <0.0001. $^{###}$Significant difference between functionalization with collagen I using either L-DOPA (*black bars*) or sulfo-SANPAH (*white bars*), p-value <0.0001. sulfo-SANPAH, sulfosuccinimidyl 6-(4′-azido-2′-nitrophenylamino)hexanoate. Color images available online at www.liebertpub.com/tec

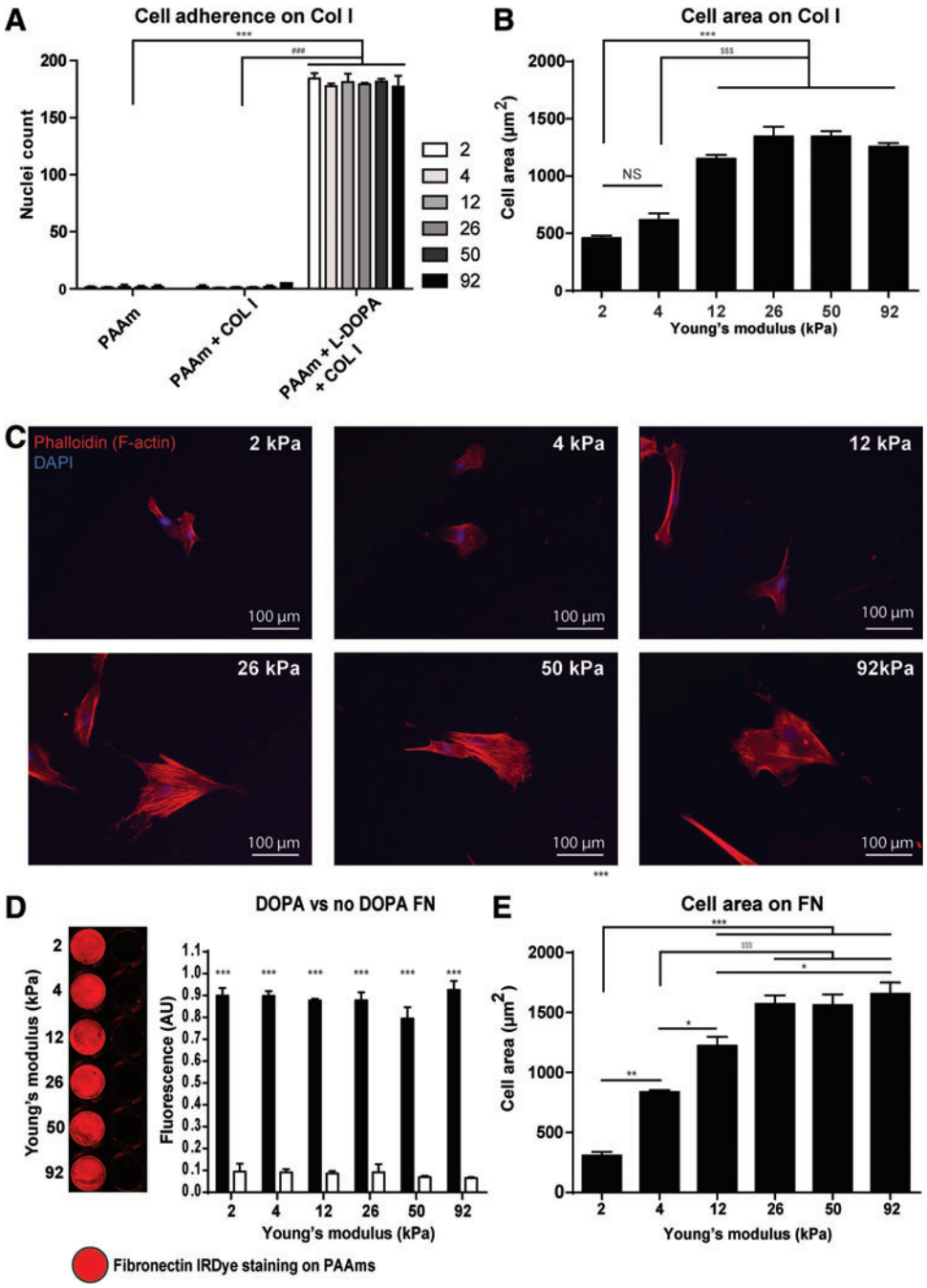

FIG. 4. Fibroblast cell area and cell adherence on PAAMs with physiological stiffness functionalized with L-DOPA and ECM. **(A)** Fibroblast cell adherence to plain PAAMs, PAAMs functionalized with only collagen I, or PAAMs functionalized with L-DOPA and collagen I. Cell adherence on plain PAAMs or PAAMs with only collagen I showed less than 3% cell adherence compared to L-DOPA and collagen I functionalized PAAMs. **(B)** Cell area as analyzed after F-actin staining with phalloidin. Cells showed marked differences in cell area, depending on PAAM stiffness ($n = 3$ for both experiments). **(C)** Fluorescence images depicting changes in cell area due to substrate stiffness on collagen I-functionalized PAAMs, original magnification 100×. **(D)** Quantification of L-DOPA–fibronectin-functionalized PAAMs using the LI-COR Odyssey infrared imaging system. Computed pseudocolored images of fibronectin coating of PAAMs are shown *left* of the quantification graph. **(E)** Cell area on L-DOPA–fibronectin-functionalized PAAMs. **(A)** ***Significant differences between PAAM alone and PAAM functionalized with L-DOPA and collagen I ($p < 0.001$). ###Significant differences between PAAM coated with only collagen I and PAAM functionalized with L-DOPA and collagen I ($p < 0.001$). **(B)** ***Significant differences in cell area between 2 and ≥12 kPa, p-value <0.001. $$$Significant difference in cell area between 4 and ≥12 kPa, p-value <0.001 **(D)** ***Significant difference in coating between L-DOPA-FN-functionalized and FN-functionalized hydrogels, p-value <0.001. **(E)** ***Significant difference in cell area between 2 and ≥12 kPa, p-value <0.001. $$$Significant different between 4 and ≥26 kPa, p-value <0.001. **Significant difference between 2 and 4 kPa, p-value <0.01. *Significant difference between 4 and 12 kPa, and between 12 and 92 kPa, p-value <0.05. FN: fibronectin. Statistics: **(A** and **D)** two-way ANOVA and **(B** and **E)** one-way ANOVA, all with Bonferroni *post hoc* analysis. Color images available online at www.liebertpub.com/tec

PAAMs with collagen type I, or PAAMs functionalized with L-DOPA and collagen type I, and cultured for 24 h. Cells hardly adhered to uncoated or collagen-coated PAAMs (without L-DOPA). Compared to L-DOPA/collagen I-functionalized hydrogels uncoated and collagen-coated PAAMs showed less than 3% cell adherence. In contrast, cells adhered homogenously to PAAMs functionalized with L-DOPA/collagen, and no significant differences in cell densities were observed between hydrogels of different stiffness (Fig. 4A). Although the quantification of cell densities between hydrogels with different stiffness revealed no differences in adhesion, significant differences were observed in cell area. Cells cultured for 48 h on PAAMs functionalized with either L-DOPA/collagen (Fig. 4B) or L-DOPA/fibronectin (Fig. 4E) showed a substrate stiffness-dependent increase in cell area. Figure 4C shows representative fluorescent images of fetal fibroblasts cultured on L-DOPA–collagen I functionalized PAAMs with different stiffness, clearly demonstrating substrate stiffness-dependent changes in cell area.

Effect of substrate stiffness on αSMA

Incorporation of αSMA into stress fibers is a well-known myofibroblast marker and is involved in, for example, cell motility, structure, integrity and contraction. Changes in cell morphology, directed by substrate stiffness, have a direct effect on αSMA localization and organization. The formation of αSMA stress fibers in fibroblasts, directed by substrate stiffness, was tested in our L-DOPA/collagen I functionalized PAAMs model. Along with changes in cell area, fetal fibroblasts

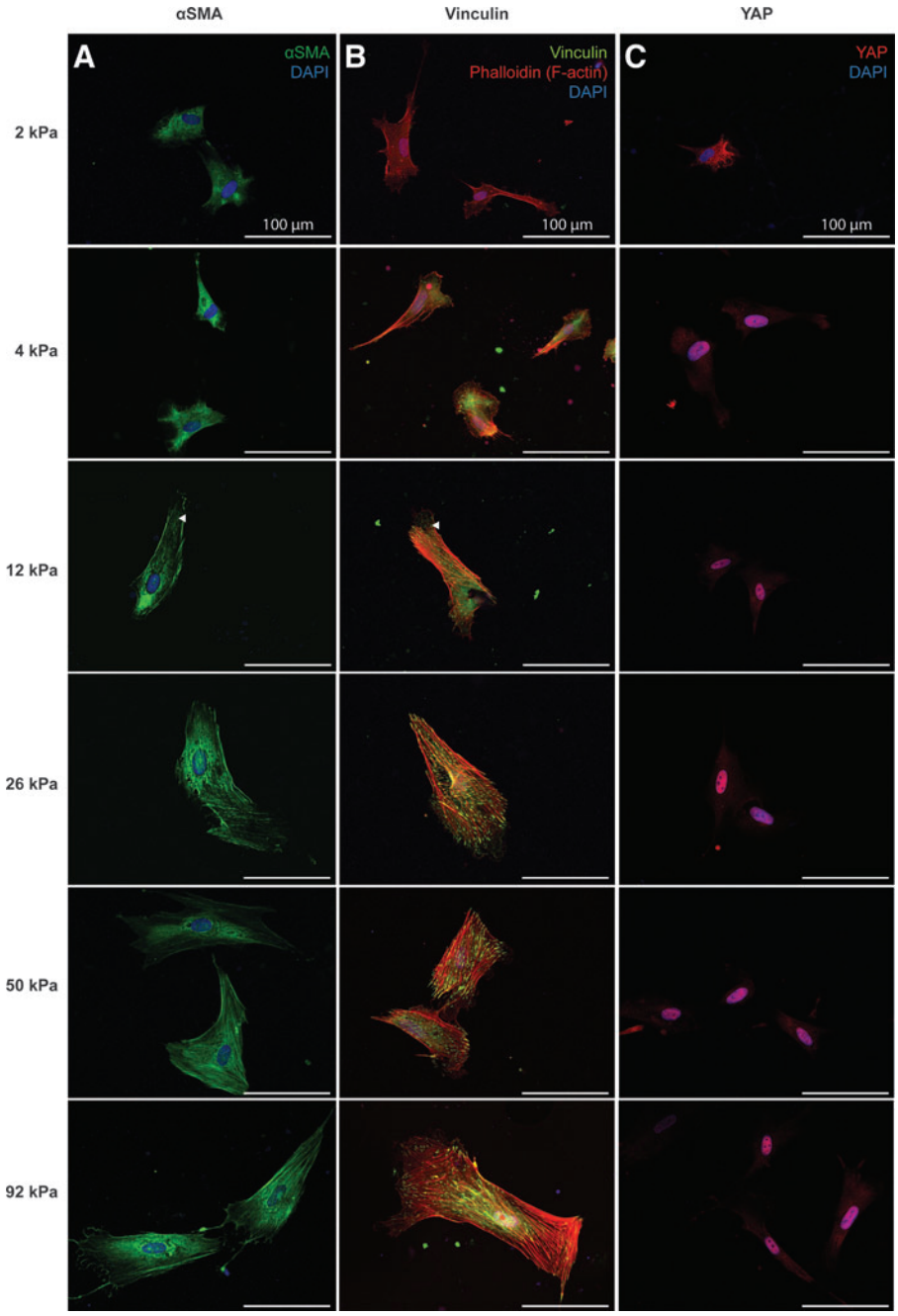

FIG. 5. Staining of three proteins known to be involved in cellular mechanosensing in fibroblasts. **(A)** Alpha smooth muscle actin (αSMA) stress fibers dissociated from stress fibers on lower substrate stiffness of 2 and 4 kPa. On substrate stiffness of 12 kPa and higher, stress fibers are formed (*arrow*). **(B)** Vinculin dissociated from focal adhesions at the lower substrate stiffness of 2 and 4 kPa. Mature focal adhesions only formed on substrate stiffness of 12 kPa and higher (*arrow*). **(C)** Yes-associated protein (YAP) was sequestered to the cytoplasm at the lowest substrate stiffness (2 kPa), but translocated to the nucleus at higher stiffness (4 kPa and higher). Original magnification 400×. Color images available online at www.liebertpub.com/tec

incorporated, as expected, αSMA into stress fibers at a stiffness of 12 kPa and higher (Fig. 5). At lower stiffness (2 and 4 kPa), αSMA dissociated from the stress fibers and was retained in the cytoplasm (Fig. 5).

Effect of substrate stiffness on vinculin localization

As the substrate stiffness has a direct effect on cellular spreading, we next validated our PAAMs with respect to the formation of focal adhesions. Vinculin, a key component in focal adhesions, plays an important role in cell–cell and cell–matrix interactions.[1,26,27] Vinculin-containing focal adhesions extend if cells sense higher stiffness and promotes cell spreading by mechanically coupling integrins to the cytoskeleton.[28–30] Singular focal adhesions also act as mechanosensors; the elongation of focal adhesions depends on the force generated by the cell on the substrate and substrate rigidity.[26,31–34] At lower stiffness values, matching physiological organ stiffness (<12 kPa), a marked decrease in focal adhesion size was observed (Fig. 5), which was accompanied by an increase in cytoplasmic vinculin staining (4 kPa) or loss of vinculin (2 kPa). In contrast, at higher stiffness we observed an increase in vinculin in focal adhesions and an increase in focal adhesion size.

Effect of substrate stiffness on YAP translocation

Cells can convert physical and mechanical signals obtained from their environment into biochemical signals. YAP, one of the main effectors of the Hippo tumor suppressor pathway, has been identified as a mechanosensing protein.[35,36]

When cells encounter a stiff matrix, YAP translocates to the nucleus and regulates gene transcription.[35,36] In our model, YAP remained cytoplasmic on 2 kPa gels but translocated to the nucleus on 4 kPa gels and stiffer (Fig. 5), which validates our model as this has also been shown by Dupont *et al.*[35]

Discussion

In this article, we propose L-DOPA[18–20] as a novel covalent linker that can functionalize the surface of PAAMs with ECM proteins. In the last decade, some researchers have shifted away from PAAMs, mainly due to its inert surface properties and problems with homogenous ECM coating when using the bifunctional cross-linker sulfo-SANPAH. In contrast, alternatives such as PDMS are less favorable for *in vitro* stiffness-based studies as they show nonlinear mechanical behavior.[17,37] Biological alternatives in the form of collagen, fibronectin, or Matrigel hydrogels fail to obtain a stiffness higher than 1 kPa unless cross-linked[38] and/or do not offer a similar surface chemistry and ECM density between gels of different stiffness, thereby convoluting stiffness and surface topography. PAAMs, however, offer linear mechanical behavior, and gels with physiological stiffness (between 1 and 100 kPa) can easily be prepared by simply varying the acryl–bisacrylamide ratio. Polyacrylamide also offers a direct positive correlation between cell spreading and bulk substrate stiffness, whereas cell spreading on PDMS is mainly influenced by the stiffness (and thickness) of the silica-like layer overlaying the cross-linked or plasma-treated PDMS surface.[39] Due to their polymer nature, all PAAMs have a homogeneous bulk substrate stiffness; all gels prepared in Table 1 were at least 100 μm in thickness, keeping in mind that a minimum threshold of 20 μm is necessary to ensure that cells only ''feel'' the gel and not the substrate (glass) below.[7,40] Although polyacrylamide gels are more suitable for studying the effect of substrate stiffness on cell mechanosensing, PDMS or other silicon derivatives might be more useful for wrinkling assays or surface modification studies.[41]

One drawback of PAAMs, hydrogel creasing, is a common but poorly defined problem in extremely soft PAAM hydrogels attached to stiff substrates (e.g., glass coverslips). Creasing can be caused by a combination of too low levels of the bisacrylamide cross-linker, osmotic pressure, and swelling.[23,42–44] As cells can enter and elongate along creases, creasing can directly influence cell morphology and behavior.[23] It is, therefore, of importance to avoid hydrogel creasing at all times when studying the effect of substrate stiffness on cellular behavior. Here, we prepared PAAMs based on the article by Saha *et al.*,[23] to ensure that no creases are formed in the gels. In brief, this means that bisacrylamide was never lowered below 0.028 wt% as this leads to PAAM instability and creases during swelling.[23]

In this article, we identified L-DOPA, the main molecular component in mussel byssus adhesion,[18,19,45] as a novel covalent linker to functionalize the inert surface of PAAMs with ECM, without introducing differences in collagen I or fibronectin density between gels with different Young's moduli. We directly compared L-DOPA with sulfo-SANPAH functionalization and reveal a significant increase in collagen I adherence to L-DOPA-coated PAAMs. L-DOPA has been used to coat a large variety of substrates, both organic and inorganic.[46] To our knowledge, this is the first time that L-DOPA is used to coat PAAM hydrogels to functionalize them with ECM components for cell culture. The exact mechanism of L-DOPA adherence to PAAMs is unknown, although both Schiff base reactions and Michaels additions have been proposed.[21] It is also known that L-DOPA can autooxidate at alkaline pH forming dopaquinone.[19,47–50] Dopaquinone offers reactive electrophilic groups at the quinone group, which can form covalent bonds with amine and thiol groups in proteins.[19] Furthermore, dopaquinone can self-polymerize forming poly-dopaquinone sheets that form multiple strong covalent and noncovalent bonds with a multitude of different organic and inorganic substrates.[19] Indeed, Lee *et al.* describe covalent interactions of oxidated dopaquinone with organic amine-coated surfaces at alkaline pH (pH 10).[19] Although the exact binding mechanism remains elusive, ECM coating on PAAMs was homogeneous, leading to homogeneous cell attachment across all functionalized PAAMs.

Fibroblasts pretreated with mitomycin C (to inhibit proliferation) adhered homogeneously on the PAAMs and showed similar cell densities between soft and stiff substrates, confirming similarity in surface chemistry and coating between gels of different substrate stiffness. Although cells showed no differences in adhesion, substrate stiffness induced marked responses in protein localization and cell area, indicating that the cells ''sense'' the stiffness of their underlying substrate below the L-DOPA and ECM layer. Solon *et al.* showed similar results with fibroblasts on PAAMs which were functionalized with sulfo-SANPAH.[51] In both our own results and Solon's article, fibroblasts have a more rounded smaller morphology and lack a clearly

defined F-actin cytoskeleton on low substrate stiffness (2 and 4 kPa), whereas at higher stiffness (12 kPa) cells spread more easily and show a neatly arranged cytoskeleton. When comparing focal adhesion sizes to a similar study conducted by Goffin *et al.*[52] on a PDMS substrate (in which the lowest substrate stiffness was 9.6 kPa), we obtained similar but more extended results. As observed by Goffin *et al.*, focal adhesion size decreases sharply below 12 kPa. We observed no focal adhesions in the lowest substrate stiffness (2 kPa) and detected mainly cytoplasmic vinculin at 4 kPa. These results could not be obtained with PDMS, as its stiffness cannot be modulated below 5 kPa, thus omitting critical physiological stiffness data points.[38]

Fibroblasts are known as mechanosensitive cells continuously probing their environment for mechanical cues and responding to changes in substrate stiffness by adapting their internal stiffness to match the stiffness of the surrounding substrate.[51] In fibroblasts, higher substrate stiffness can lead to more internal tension, high contraction, and formation of αSMA stress fibers.[51,53] One way to match the internal stiffness to the softer surrounding substrate is by remodeling the cytoskeleton, which in turn leads to a smaller cell area and less intracellular tension. αSMA stress fibers and focal adhesions increase due to enhanced intracellular tension[54] and focal adhesions quickly disassociate after loss of intracellular tension.[55–59] On lower stiffness hydrogels, fibroblasts have less internal tension, are less contractile, and disassemble αSMA stress fibers.[53] In our experiments, incorporation of αSMA in stress fibers and vinculin-positive focal adhesions was only observed at stiffness higher than 4 kPa, matching results from other groups.[3,52] Last, to validate our system, we studied YAP localization. YAP is involved in mechanosensitive translocation to the nucleus and is only retained in the cytoplasm if internal tension is low. Similar to results obtained by Dupont *et al.*, YAP retained in the cytoplasm only on the lowest substrate stiffness. On higher stiffness (4 kPa and higher), YAP translocated to the nucleus, where it can interact with transcription factors and modulate differentiation and proliferation.[35]

Conclusions

We conclude that L-DOPA is a nontoxic and biocompatible[22] cross-linker that can be used to more easily, more homogeneously, and more efficiently functionalize PAAMs with ECM components when compared to sulfo-SANPAH. With this straightforward *in vitro* model, the effect of substrate stiffness on cell mechanosensing and mechanotransduction can be studied, without the drawbacks of sulfo-SANPAH and other cross-linkers.

Acknowledgments

The authors gratefully acknowledge the financial support of The Netherlands Institute for Regenerative Medicine, the Kolff Graduate School, and the J.K. de Cock Foundation. Special thanks are due to Joop de Vries of the Biomedical Engineering Department of the University of Groningen for use of the AFM and technical support.

Disclosure Statement

No competing financial interests exist.

References

1. Ingber, D.E. Cellular mechanotransduction: putting all the pieces together again. FASEB J **20,** 811, 2006.
2. Discher, D.E., Janmey, P., and Wang, Y.-L. Tissue cells feel and respond to the stiffness of their substrate. Science **310,** 1139, 2005.
3. Yeung, T., Georges, P.C., Flanagan, L.A., Marg, B., Ortiz, M., Funaki, M., *et al.* Effects of substrate stiffness on cell morphology, cytoskeletal structure, and adhesion. Cell Motil Cytoskeleton **60,** 24, 2005.
4. Pelham, R.J., and Wang, Y.L. Cell locomotion and focal adhesions are regulated by the mechanical properties of the substrate. Biol Bull **194,** 348, 1998.
5. Lo, C.M., Wang, H.B., Dembo, M., and Wang, Y.L. Cell movement is guided by the rigidity of the substrate. Biophys J **79,** 144, 2000.
6. Wang, H., Dembo, M., and Wang, Y. Substrate flexibility regulates growth and apoptosis of normal but not transformed cells. Am J Physiol Cell Physiol **279,** C1345, 2013.
7. Engler, A.J., Sen, S., Sweeney, H.L., and Discher, D.E. Matrix elasticity directs stem cell lineage specification. Cell **126,** 677, 2006.
8. Engler, A.J., Griffin, M.A., Sen, S., Bönnemann, C.G., Sweeney, H.L., and Discher, D.E. Myotubes differentiate optimally on substrates with tissue-like stiffness: pathological implications for soft or stiff microenvironments. J Cell Biol **166,** 877, 2004.
9. Pelham, R.J., and Wang, Y.-L. Cell locomotion and focal adhesions are regulated by substrate flexibility. Proc Natl Acad Sci U S A **94,** 13661, 1997.
10. Wang, Y.L., and Pelham, R.J. Preparation of a flexible, porous polyacrylamide substrate for mechanical studies of cultured cells. Methods Enzymol **298,** 489, 1998.
11. Beningo, K.A., and Wang, Y. Fc-receptor-mediated phagocytosis is regulated by mechanical properties of the target. J Cell Sci **115,** 849, 2002.
12. Storm, C., Pastore, J.J., MacKintosh, F.C., Lubensky, T.C., and Janmey, P.A. Nonlinear elasticity in biological gels. Nature **435,** 191, 2005.
13. Domke, J., and Radmacher, M. Measuring the elastic properties of thin polymer films with the atomic force microscope. Langmuir **14,** 3320, 1998.
14. Sneddon, I.N. The relation between load and penetration in the axisymmetric boussinesq problem for a punch of arbitrary profile. Int J Eng Sci **3,** 47, 1965.
15. Tse, J.R., and Engler, A.J. Preparation of hydrogel substrates with tunable mechanical properties. Curr Protoc Cell Biol **10,** 1, 2010.
16. Kandow, C.E., Georges, P.C., Janmey, P.A., and Beningo, K.A. Polyacrylamide hydrogels for cell mechanics: steps toward optimization and alternative uses. Methods Cell Biol **83,** 29, 2007.
17. Huang, R.C., and Anand, L. Non-linear mechanical behavior of the elastomer polydimethylsiloxane (PDMS) used in the manufacture of microfluidic devices. Innov Manuf Syst Technol **1,** 1, 2005.
18. Waite, J.H., and Tanzer, M.L. The bioadhesive of Mytilus byssus: a protein containing L-dopa. Biochem Biophys Res Commun **96,** 1554, 1980.
19. Lee, H., Scherer, N.F., and Messersmith, P.B. Single-molecule mechanics of mussel adhesion. Proc Natl Acad Sci U S A **103,** 12999, 2006.

20. Li, Y.Y., Qin, M., Li, Y.Y., Cao, Y., and Wang, W. Single molecule evidence for the adaptive binding of DOPA to different wet surfaces. Langmuir **30,** 4358, 2014.
21. Lee, H., Dellatore, S., Miller, W., and Messersmith, P.B. Mussel-inspired surface chemistry for multifunctional coatings. Science **318,** 426, 2007.
22. La, W.G., Bhang, S.H., Shin, J.-Y.Y., Yoon, H.H., Park, J., Yang, H.S., *et al.* 3,4-dihydroxy-L-phenylalanine as a cell adhesion molecule in serum-free cell culture. Biotechnol Prog **28,** 1055, 2012.
23. Saha, K., Kim, J., Irwin, E., Yoon, J., Momin, F., Trujillo, V., *et al.* Surface creasing instability of soft polyacrylamide cell culture substrates. Biophys J **99,** 94, 2010.
24. Pelham, R.J., and Wang, Y.L. High resolution detection of mechanical forces exerted by locomoting fibroblasts on the substrate. Mol Biol Cell **10,** 935, 1999.
25. Schindelin, J., Arganda-Carreras, I., Frise, E., Kaynig, V., Longair, M., Pietzsch, T., *et al.* Fiji: an open source platform for biological image analysis. Nat Methods **9,** 676, 2012.
26. Bershadsky, A.D., Ballestrem, C., Carramusa, L., Zilberman, Y., Gilquin, B., Khochbin, S., *et al.* Assembly and mechanosensory function of focal adhesions: experiments and models. Eur J Cell Biol **85,** 165, 2006.
27. Chen, C.S., Tan, J., and Tien, J. Mechanotransduction at cell-matrix and cell-cell contacts. Annu Rev Biomed Eng **6,** 275, 2004.
28. Spanjaard, E., and De Rooij, J. Mechanotransduction: vinculin provides stability when tension rises. Curr Biol **23,** R159, 2013.
29. Ezzell, R.M., Goldmann, W.H., Wang, N., Parashurama, N., and Ingber, D.E. Vinculin promotes cell spreading by mechanically coupling integrins to the cytoskeleton. Exp Cell Res **231,** 14, 1997.
30. Schoenwaelder, S.M., and Burridge, K. Bidirectional signaling between the cytoskeleton and integrins. Curr Opin Cell Biol **11,** 274, 1999.
31. Riveline, D., Zamir, E., Balaban, N.Q., Schwarz, U.S., Ishizaki, T., Narumiya, S., *et al.* Focal contacts as mechanosensors: externally applied local mechanical force induces growth of focal contacts by an mDia1-dependent and ROCK-independent mechanism. J Cell Biol **153,** 1175, 2001.
32. Bershadsky, A.D., Balaban, N.Q., and Geiger, B. Adhesion-dependent cell mechanosensitivity. Annu Rev Cell Dev Biol **19,** 677, 2003.
33. Geiger, B., and Bershadsky, A. Exploring the neighborhood: adhesion-coupled cell mechanosensors. Cell **110,** 139, 2002.
34. Balaban, N.Q., Schwarz, U.S., Riveline, D., Goichberg, P., Tzur, G., Sabanay, I., *et al.* Force and focal adhesion assembly: a close relationship studied using elastic micropatterned substrates. Nat Cell Biol **3,** 466, 2001.
35. Dupont, S., Morsut, L., Aragona, M., Enzo, E., Giulitti, S., Cordenonsi, M., *et al.* Role of YAP/TAZ in mechanotransduction. Nature **474,** 179, 2011.
36. Calvo, F., Ege, N., Grande-Garcia, A., Hooper, S., Jenkins, R.P., Chaudhry, S.I., *et al.* Mechanotransduction and YAP-dependent matrix remodelling is required for the generation and maintenance of cancer-associated fibroblasts. Nat Cell Biol **15,** 637, 2013.
37. Kim, H.T., and Jeong, O.C. Measurement of nonlinear mechanical properties of surfactant-added poly(dimethylsiloxane). Jpn J Appl Phys 51, 06FK07, 2012.
38. Rehfeldt, F., Engler, A.J., Eckhardt, A., Ahmed, F., and Discher, D.E. Cell responses to the mechanochemical microenvironment—implications for regenerative medicine and drug delivery. Adv Drug Deliv Rev **59,** 1329, 2007.
39. Li, J., Han, D., and Zhao, Y.-P. Kinetic behaviour of the cells touching substrate: the interfacial stiffness guides cell spreading. Sci Rep **4,** 3910, 2014.
40. Lee, S., Zeiger, A., Maloney, J.M., Kotecki, M., van Vliet, K.J., and Herman, I.M. Pericyte actomyosin-mediated contraction at the cell-material interface can modulate the microvascular niche. J Phys Condens Matter **22,** 194115, 2010.
41. Harris, A.K., Wild, P., and Stopak, D. Silicone rubber substrata: a new wrinkle in the study of cell locomotion. Science **208,** 177, 1980.
42. Dervaux, J., and Amar, M.B. Mechanical instabilities of gels. Annu Rev Condens Matter Phys **3,** 311, 2012.
43. Kang, M.K., and Huang, R. Swell-induced surface instability of confined hydrogel layers on substrates. J Mech Phys Solids **58,** 1582, 2010.
44. Trujillo, V., Kim, J., and Hayward, R.C. Creasing instability of surface-attached hydrogels. Soft Matter **4,** 564, 2008.
45. Lee, H. Biomaterials: intelligent glue. Nature **465,** 298, 2010.
46. Guvendiren, M., Brass, D.A., Messersmith, P.B., and Shull, K.R. Adhesion of DOPA-functionalized model membranes to hard and soft surfaces. J Adhes **85,** 631, 2009.
47. Herlinger, E., Jameson, R.F., and Linert, W. Spontaneous autoxidation of dopamine. J Chem Soc Perkin Trans 2 259, 1995.
48. Faure, E., Falentin-Daudré, C., Jérôme, C., Lyskawa, J., Fournier, D., Woisel, P., *et al.* Catechols as versatile platforms in polymer chemistry. Prog Polym Sci **38,** 236, 2013.
49. Faure, E., Lecomte, P., Lenoir, S., Vreuls, C., Van De Weerdt, C., Archambeau, C., *et al.* Sustainable and bio-inspired chemistry for robust antibacterial activity of stainless steel. J Mater Chem **21,** 7901, 2011.
50. Burzio, L.A., and Waite, J.H. Cross-linking in adhesive quinoproteins: studies with model decapeptides. Biochemistry **39,** 11147, 2000.
51. Solon, J., Levental, I., Sengupta, K., Georges, P.C., and Janmey, P.A. Fibroblast adaptation and stiffness matching to soft elastic substrates. Biophys J **93,** 4453, 2007.
52. Goffin, J.M., Pittet, P., Csucs, G., Lussi, J.W., Meister, J.J., and Hinz, B. Focal adhesion size controls tension-dependent recruitment of α-smooth muscle actin to stress fibers. J Cell Biol **172,** 259, 2006.
53. Godbout, C., Follonier Castella, L., Smith, E.A., Talele, N., Chow, M.L., Garonna, A., *et al.* The mechanical environment modulates intracellular calcium oscillation activities of myofibroblasts. PLoS One **8,** e64560, 2013.
54. Ridley, A.J., and Hall, A. The small GTP-binding protein rho regulates the assembly of focal adhesions and actin stress fibers in response to growth factors. Cell **70,** 389, 1992.
55. Helfman, D.M., Levy, E.T., Berthier, C., Shtutman, M., Riveline, D., Grosheva, I., *et al.* Caldesmon inhibits nonmuscle cell contractility and interferes with the formation of focal adhesions. Mol Biol Cell **10,** 3097, 1999.

56. Chrzanowska-Wodnicka, M., and Burridge, K. Rho-stimulated contractility drives the formation of stress fibers and focal adhesions. J Cell Biol **133,** 1403, 1996.
57. Burridge, K., and Chrzanowska-Wodnicka, M. Focal adhesions, contractility, and signaling. Annu Rev Cell Dev Biol **12,** 463, 1996.
58. Kaverina, I., Krylyshkina, O., and Small, J.V. Microtubule targeting of substrate contacts promotes their relaxation and dissociation. J Cell Biol **146,** 1033, 1999.
59. Volberg, T., Geiger, B., Citi, S., and Bershadsky, A.D. Effect of protein kinase inhibitor H-7 on the contractility, integrity, and membrane anchorage of the microfilament system. Cell Motil Cytoskeleton **29,** 321, 1994.

Address correspondence to:
Ruud A. Bank, PhD
Department of Pathology and Medical Biology
University of Groningen
University Medical Center Groningen
Hanzeplein 1
Groningen 9713 GZ
The Netherlands

E-mail: r.a.bank@umcg.nl

Received: July 1, 2015
Accepted: November 2, 2015
Online Publication Date: January 5, 2016